Inorganic Chemistry

Article

pubs.acs.org/IC

Crystal Structure and Solution Species of Ce(III) and Ce(IV) Formates: From Mononuclear to Hexanuclear Complexes

Christoph Hennig,*[,†,‡] Atsushi Ikeda-Ohno,[†,§,∥] Werner Kraus,[⊥] Stephan Weiss,[†] Philip Pattison,[⊗] Hermann Emerich,[⊗] Paula M. Abdala,[⊗] and Andreas C. Scheinost[†,‡]

[†]Helmholtz-Zentrum Dresden-Rossendorf, Institute of Resource Ecology, Bautzner Landstrasse 400, D-01314 Dresden, Germany

[‡]The Rossendorf Beamline, ESRF, BP 220, F-38043 Grenoble, France

[§]School of Civil and Environmental Engineering, The University of New South Wales, UNSW, Sydney, NSW 2052, Australia

[∥]Institute for Environmental Research, Australian Nuclear Science and Technology Organisation, Locked Bag 2001, Kirrawee DC, New South Wales 2232, Australia

[⊥]BAM Federal Institute for Materials Research and Testing, Richard-Willstätter-Strasse 11, D-12489 Berlin, Germany

[⊗]Swiss−Norwegian Beamlines, ESRF, BP 220, F-38043 Grenoble, France

Supporting Information

ABSTRACT: Cerium(III) and cerium(IV) both form formate complexes. However, their species in aqueous solution and the solid-state structures are surprisingly different. The species in aqueous solutions were investigated with Ce K-edge EXAFS spectroscopy. Ce(III) formate shows only mononuclear complexes, which is in agreement with the predicted mononuclear species of $Ce(HCOO)^{2+}$ and $Ce(HCOO)_2^{+}$. In contrast, Ce(IV) formate forms in aqueous solution a stable hexanuclear complex of $[Ce_6(\mu_3\text{-}O)_4(\mu_3\text{-}OH)_4(HCOO)_x(NO_3)_y]^{12-x-y}$. The structural differences reflect the different influence of hydrolysis, which is weak for Ce(III) and strong for Ce(IV). Hydrolysis of Ce(IV) ions causes initial polymerization while complexation through $HCOO^-$ results in 12 chelate rings stabilizing the hexanuclear Ce(IV) complex. Crystals were grown from the above-mentioned solutions. Two crystal structures of Ce(IV) formate were determined. Both form a hexanuclear complex with a $[Ce_6(\mu_3\text{-}O)_4(\mu_3\text{-}OH)_4]^{12+}$ core in aqueous HNO_3/HCOOH solution. The pH titration with NaOH resulted in a structure with the composition $[Ce_6(\mu_3\text{-}O)_4(\mu_3\text{-}OH)_4(HCOO)_{10}(NO_3)_2(H_2O)_3]\cdot(H_2O)_{9.5}$, while the pH adjustment with NH_3 resulted in $[Ce_6(\mu_3\text{-}O)_4(\mu_3\text{-}OH)_4(HCOO)_{10}(NO_3)_4]\cdot(NO_3)_3(NH_4)_5(H_2O)_5$. Furthermore, the crystal structure of Ce(III) formate, $Ce(HCOO)_3$, was determined. The coordination polyhedron is a tricapped trigonal prism which is formed exclusively by nine $HCOO^-$ ligands. The hexanuclear Ce(IV) formate species from aqueous solution is widely preserved in the crystal structure, whereas the mononuclear solution species of Ce(III) formate undergoes a polymerization during the crystallization process.

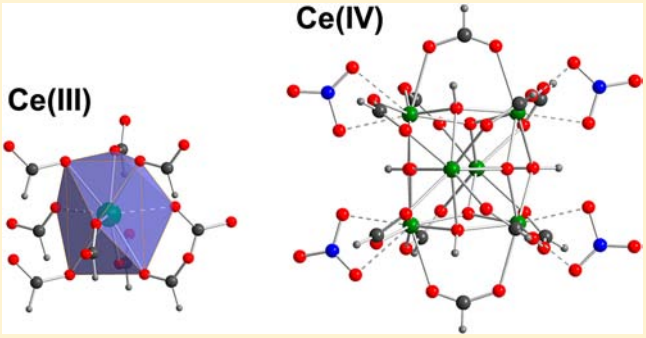

1. INTRODUCTION

A characteristic feature of the lanthanide elements (Ln) in aqueous solution is the dominant formation of stable trivalent cations, Ln^{3+}. There are only a few exceptions to this rule. One example is Ce^{4+}, which is considered as the only lanthanide forming stable tetravalent ions in aqueous solution.[1] The stability of Ce^{4+} ion originates in its $[Xe]f^0$ electron configuration. In general, the Ce^{3+} ion is the thermodynamically most stable form in aqueous solution. The Ce^{4+} ion is kinetically stabilized, usually by anion complexation, showing little deterioration over several months.[2] Ce(III) cannot be oxidized to Ce(IV) by molecular oxygen but through electrolysis or strong oxidizing agents such as ozone.

In aqueous solution the Ce^{3+} ion is strongly hydrated because of its high charge to ionic radius ratio. As one of the lighter lanthanides, Ce^{3+} generally forms a mononuclear nonahydrated aqua complex, $Ce(H_2O)_9^{3+}$, whereas the heavier lanthanides show 8-fold hydration.[3,4] The hydrolysis of Ce^{3+} is relatively weak. In contrast, the Ce^{4+} ion shows a strong tendency toward hydrolysis.[5] Because of this strong hydrolysis, small oligomers occur through hydrolytic polymerization even in highly acidic media[5,6] and colloidal CeO_2 nanocrystals are further formed at moderate acidic condition.[7] The variety of hydrates and hydrolysis species between Ce^{3+} and Ce^{4+} contributes to the wide variation of the redox potential values (E^0) reported for the Ce^{3+}/Ce^{4+} couples in various media.[8,9]

Ce^{3+} and Ce^{4+} both readily undergo complexation with carboxylic ligands.[1,10] Formate, $HCOO^-$, the anion derived from formic acid, is the simplest carboxylic ligand whose

Received: April 22, 2013
Published: October 3, 2013

   dx.doi.org/10.1021/ic400999j | Inorg. Chem. 2013, 52, 11734−11743

chemical character is strongly determined by the carboxylic group.[11] Formic acid is miscible with water at any ratio because of the polar character of the carboxylic group. Formate acts as an important intermediate of metabolism in bacteria and as preliminary carrier of carbon dioxide.[12] Formic acid is considered as one of the most promising materials for hydrogen storage in fuel cells.[13] CeO_2 belongs to a family of catalysts employed to decompose formic acid in such fuel cells to release hydrogen.[14] The adsorption of formic acid onto the CeO_2 catalyst has been reported to proceed through formation of a bidentate bridge between two neighboring Ce atoms.[15]

One of the most important applications of the chemistry of cerium carboxylate complexes is in the area of organic synthesis. For instance, ceric ammonium nitrate (CAN, $(NH_4)_2Ce(NO_3)_6$) is one of the most frequently used reagents to produce carboxylate compounds from alcohols.[16] Moreover, it is often employed in carboxylic acid media for synthesizing other organic compounds.[16] Another emerging application of carboxylate-related complexes of cerium is its use as an artificial site-selective DNA cutter, which hydrolyzes single-stranded DNA at a desired site.[17] These applications require a fundamental knowledge of cerium carboxylate complexes to understand the actual chemical processes occurring in the systems, which is indispensable to further developments. Based on this background, formate is an appropriate ligand to study the coordination chemistry of cerium carboxylate complexes particularly in aqueous solutions.

For Ce(III) formate in aqueous solution, two stability constants are reported: $Ce(HCOO)^{2+}$, $\log \beta_1 = 1.79$ and $Ce(HCOO)_2^{+}$ with $\log \beta_2 = 2.97$.[10,18−20] However, no structural data are reported on Ce(III) formate complexes in solution so far. Besides, there is no single-crystal X-ray diffraction data reporting the structure of the Ce(III) formate. Only one study reports neutron powder diffraction data of the deuterated compound of $Ce(DCOO)_3$ whose structure was estimated in analogy to other isostructural Ln(III) formats.[21] Another study reports single-crystal X-ray diffraction of a mixed compound, $Ce_{0.9}Gd_{0.1}(HCOO)_3$, which is isostructural to $Ce(DCOO)_3$.[22] To the best of our knowledge, there are no stability constants available in the literature for Ce(IV) formate. Furthermore, there are neither crystal structures of Ce(IV) formate published nor are there structural data of the relevant solution species.

2. EXPERIMENTAL SECTION

2.1. Sample Preparation. *Aqueous Solutions.* The liquid samples, their pH, and the sample-ID are summarized in Table 1.

Ce(III) formate. An aqueous solution of Ce(III) formate was prepared by dissolving 50 mg of $Ce(HCOO)_3$ in 10 mL of deionized water (sample **A2**). $Ce(HCOO)_3$ was taken from the later described solid sample **P1**. The pH value approached 5.74 without further adjustment. A reference sample with the pure Ce(III) aquo species, $Ce^{3+}(aq)$, was prepared by dissolving 434 mg of $Ce(NO_3)_3{\cdot}6H_2O$ (>98.5%, Merck) to achieve a solution with 0.1 M Ce(III) in 10 mL of deionized water (sample **A1**). The pH was adjusted at 2.0 with 0.1 M HNO_3.

Ce(IV) formate. A weighed amount of $Ce(NO_3)_3{\cdot}6H_2O$ (99.99%, Merck) was dissolved into aqueous HNO_3 to give a 0.12 M Ce(III) solution in 0.56 M HNO_3. This solution was purged by bubbling N_2 gas for 3 h to remove dissolved oxygen and then electrolyzed at 1.9 V to oxidize Ce(III) to Ce(IV) by using a potentiostat (Metrohm Autolab PGSTAT12/30/302) with a three electrode system (Pt-plate working and counter electrodes, and a Ag/AgCl reference electrode in 3 M NaCl).

Table 1. List of Ce(III) and Ce(IV) Samples in Solution

sample ID	solution composition	pH
A1	0.1 M $Ce(III)(NO_3)_3{\cdot}6H_2O$ in H_2O	2.0
A2	0.018 M $Ce(III)(HCOO)_3$ in H_2O	5.74
Init	0.12 M Ce(IV) in 0.56 M HNO_3	*a*
F1	0.1 M Ce(IV) in 0.5 M HNO_3/1.0 M HCOOH	1.60[b]
F2	0.1 M Ce(IV) in 0.5 M HNO_3/1.0 M HCOOH	1.23
F3	0.1 M Ce(IV) in 0.5 M HNO_3/1.0 M HCOOH	0.88
F4	0.1 M Ce(IV) in 0.5 M HNO_3/1.0 M HCOOH	0.60
F5	0.1 M Ce(IV) in 0.5 M HNO_3/1.0 M HCOOH	0.66
F6	0.1 M Ce(IV) in 0.5 M HNO_3/1.0 M HCOOH	0.83
F7	0.1 M Ce(IV) in 0.5 M HNO_3/1.0 M HCOOH	1.16
F8	0.1 M Ce(IV) in 0.5 M HNO_3/1.0 M HCOOH	1.56
F9	0.1 M Ce(IV) in 0.5 M HNO_3/1.0 M HCOOH	2.05
F10	0.1 M Ce(IV) in 0.5 M HNO_3/1.0 M HCOOH	3.50

[a]The pH value of this sample depends on the duration of the electrolysis. [b]Sample **F1** results from sample **Init** by adding HCOOH without pH adjustment. The pH values of the subsequent samples were adjusted with NH_3.

An 18 mL portion of the 0.12 M Ce(IV) solution in 0.56 M HNO_3 was mixed with 2.0 mL of 10 M HCOOH to give 0.1 M Ce(IV), 0.5 M HNO_3, and 1 M HCOOH. The resultant solution (sample **Init**) was employed as a stock solution for subsequent pH titration experiments. The stock solution was sequentially titrated by a NH_3 solution (25%, Merck) to prepare a series of Ce(IV) solution samples with different pH values. At each pH, a 1 mL of the titrated solution was collected for XAFS samples. The pH measurement was performed by using a pH meter (inoLab WTW-pH720) calibrated with four different pH buffer solutions (pH = 1.68, 4.01, 6.86, and 9.18 at 298 K). All sample preparation and sealing were performed in an inert glovebox filled with N_2 to avoid the penetration of atmospheric oxygen or carbon dioxide into the sample solutions. Additionally, deionized water used for sample preparation was degassed and deoxygenated by purging N_2 prior to its use. The electrochemically prepared Ce(IV) solutions were employed for single crystal preparation.

Solid Compounds. $Ce(HCOO)_3$ (sample **1**). Several attempts were made to obtain single crystals of $Ce(HCOO)_3$. Attempts to crystallize the compound directly from a aqueous solution of Ce(III) formate resulted only in powder samples. Single crystals of $Ce(HCOO)_3$ were obtained from a solution of 1.0 M Ce(IV), 1.0 M HNO_3/10.0 M HCOOH (initial pH = 0.8 adjusted with NH_3) which underwent slow photoreduction of Ce(IV) to Ce(III). The single crystals were deposited after 6 months in the sealed vial without evaporation under ambient conditions.

$Ce(HCOO)_3$ (microcrystalline powder, sample **P1**). One-hundred mg of $CeCl_3 \times 7\ H_2O$ (Laborchemie Apolda, p.a. grade) was dissolved in 10 mL of diethylene glycol monoethyl ether (Merck, synthesis grade). A white precipitate was formed after addition of 40 μL of 98−100% formic acid (Merck, p.a. grade) and 200 μL of 25% NH_3 (Merck, p.a. grade). The solid precipitate was washed two times with diethylene glycol monoethyl ether and one time with diethyl ether and dried at air. The powder X-ray diffraction (XRD) pattern, shown in the Supporting Information, Figure S1, is in agreement with the lattice parameters of compound **1**.

$[Ce_6(\mu_3\text{-}O)_4(\mu_3\text{-}OH)_4(HCOO)_{10}(NO_3)_2(H_2O)_3]{\cdot}(H_2O)_{9.5}$ (sample **2**). A yellow colored solution of 1.0 M Ce(IV) in 1.0 M HNO_3/10.0 M HCOOH (pH = 0.2 adjusted with NaOH) was centrifuged with 3,500 rpm for 10 min, and the supernatant solution was transferred into a plastic tube. Slow evaporation of the solution for several days under ambient conditions yielded clear yellow crystals. A powder diffraction pattern of the sample shows only the presence of one crystal structure (Supporting Information, Figure S2). Anal. Calcd for $C_{10}H_{39}Ce_6N_2O_{46.5}$: Ce, 47.4; C, 6.8; H, 2.2; N, 1.6; O, 42.0. Found: Ce, 48.3; C, 6.6; H, 2.1; N, 1.7; O 41.6. IR (KBr) ν_{max} (cm^{-1}): 3431 (b, H_2O), 1583 (b), 1481 (b), 1384 (m), 1357 (b), 1280 (w), 1031 (b), 811 (s), 781 (w), 748 (s), 553 (s), 428 (w), 407 (vw).

dx.doi.org/10.1021/ic400999j | Inorg. Chem. 2013, 52, 11734−11743

$[Ce_6(\mu_3\text{-}O)_4(\mu_3\text{-}OH)_4(HCOO)_{10}(NO_3)_4]\cdot(NO_3)_3(NH_4)_5(H_2O)_5$ (sample **3**). A yellow colored solution of 1.0 M Ce(IV) in 1.0 M HNO_3/10.0 M HCOOH (pH = 0.5 adjusted with NH_3) was centrifuged with 3,500 rpm for 10 min. The supernatant solution was transferred into a plastic tube and evaporated slowly under ambient conditions. Clear yellow crystals were deposited after several days of the evaporation. A powder diffraction pattern of the sample shows only the presence of one crystal structure (Supporting Information, Figure S3). Anal. Calcd for $C_{10}H_{44}Ce_6N_{12}O_{54}$: Ce, 41.3; C, 5.9; H, 2.2; N, 8.2; O, 42.4. Found: Ce, 37.1; C, 5.8; H, 2.3; N, 8.3; O, 41.5. IR (KBr) ν_{max} (cm^{-1}): 3400 (b, H_2O), 3240 (b, NH_4), 1583 (b), 1469 (w), 1429 (s), 1385 (s), 1358 (m), 1098 (s), 1037 (s), 831 (s), 810 (s), 781 (s), 744 (s), 553 (s), 442 (w), 409 (vw).

2.2. Crystal Structure and Spectroscopic Characterization. *X-ray Diffraction.* The single crystal X-ray data collection was carried out on a Bruker AXS SMART diffractometer at room temperature using Mo Kα radiation (λ = 0.71073 Å) monochromatized by a graphite crystal. Data reduction was performed by using the Bruker AXS SAINT and SADABS packages. The structures were solved by direct methods and refined by full-matrix least-squares calculation using SHELX.[23] Anisotropic thermal parameters were employed for non-hydrogen atoms. The hydrogen atoms were treated isotropically with U_{iso} =1.2 times the U_{eq} value of the parent atom. Only the hydrogen atom from compound **1** was found in the difference Fourier map and fixed with restraints for bond length and angles. The hydrogen atoms included in the cluster were introduced in ideal positions. The protons of H_2O and NH_4^+ anions could not be located in the difference Fourier map. Crystal data and refinement details are summarized in Table 2. The crystallographic data for the structures have been deposited with the Cambridge Crystallographic Data Centre. The CCDC numbers are listed in Table 2. Copies of the data can be obtained, free of charge, on application to CCDC, 12 Union Road, Cambridge CB2 1EZ, U.K., fax: +44 1223 336033 or e-mail: deposit@ccdc.cam.ac.uk.

Table 2. Summary of Crystallographic Data and Structure Refinement Details for Compounds 1, 2, and 3

	1	2	3
chemical formula	$C_3H_3CeO_6$	$C_{10}H_{39}Ce_6N_2O_{46.5}$	$C_{10}H_{44}Ce_6N_{12}O_{54}$
formula mass	275.17	1746.95	2007.05
crystal system	trigonal	monoclinic	orthorhombic
a/Å	10.706(2)	12.3326(10)	12.3752(17)
b/Å	10.706(2)	19.5209(16)	26.152(3)
c/Å	4.1205(12)	18.9260(16)	15.698(3)
α/deg	90.00	90.00	90.00
β/deg	90.00	108.313(4)	90.00
γ/deg	120.00	90.00	90.00
unit cell volume/Å^3	409.01(18)	4325.6(6)	5080.4(13)
temperature/K	296(2)	296(2)	296(2)
Space group	*R*3*m*	$P2_1/c$	*Pbcn*
No. of formula units per unit cell, Z	3	4	4
radiation type	MoKα	MoKα	MoKα
absorption coefficient, μ/mm^{-1}	8.311	6.314	5.410
no. of reflections measured	1780	61601	5054
no. of independent reflections	264	11248	5054
R_{int}	0.1116	0.1197	0.0000
final R_1 values ($I > 2\sigma(I)$)	0.0325	0.0468	0.0347
final $wR(F^2)$ values ($I > 2\sigma(I)$)	0.0741	0.1190	0.1049
final R_1 values (all data)	0.0325	0.0604	0.0427
final $wR(F^2)$ values (all data)	0.0741	0.1245	0.1116
goodness of fit on F^2	1.176	1.035	1.291
CCDC no.	925639	925637	925638

EXAFS Measurements. EXAFS measurements were performed in transmission mode using a Si(111) double-crystal monochromator at the Swiss–Norwegian Beamlines at the European Synchrotron Radiation Facility (Grenoble, France). Ce K-edge spectra were collected using ionization chambers filled with 25% krypton and 80% nitrogen before the sample (I_0) and with pure krypton after the sample (I_1, I_2) at ambient temperature and pressure. CeO_2 was used for energy calibration. The Ce K-edge threshold energy, $E_{k=0}$, was set to 40.447 keV at the first inflection point of the Ce absorption edge. EXAFS data were extracted from the raw absorption spectra by standard methods including a spline approximation for the atomic background using the programs WINXAS[24] and EXAFSPAK.[25] Theoretical phase and amplitude functions were calculated with FEFF 8.20[26] by using atomic parameters of the crystal structures obtained in this study, and structures described in the Supporting Information, Figures S11 and S13. The FT peaks are shifted to lower values $R + \Delta$ relative to the true near-neighbor distances R because of the phase shift of the electron wave in the adjacent atomic potentials. This Δ shift is considered as a variable during the shell fits. The amplitude reduction factor, S_0^2, was defined as 0.9 and fixed to that value in the data fits. A series of solution samples was analyzed by iterative target transformation factor analysis using the ITFA program.[27a] The standard deviations of the relative concentrations were determined with the algorithm from ref 27b.

XANES Measurements. Ce L_3-edge XANES measurements were performed using a Si(111) double-crystal monochromator on the Rossendorf Beamline at the European Synchrotron Radiation Facility (Grenoble, France). Higher harmonics were rejected by two Si coated mirrors. The spectra were collected using ionization chambers filled with nitrogen and a Ge fluorescence detector at ambient temperature and pressure. The Ce L_3 energy was calibrated against the first strong peak at 5.725 keV in the XANES spectrum of an aqueous Ce(III) solution with 0.01 M $Ce(NO_3)_3\cdot 6H_2O$.

Chemical Analysis. The concentration of Ce was measured after acidic sample digestion by inductively coupled plasma mass spectrometry (ICP/MS) with an ELAN 5000 type spectrometer (Perkin-Elmer, Germany) with an error of 5%. Elemental analysis was performed by a CHNO Rapid Elemental Analyzer (Heraeus, Hanau, Germany) with error limits of C ± 0.3, H ± 0.2, N ± 0.4, O ± 1.0. IR spectra were recorded with a Bruker Vertex 80/v spectrometer with a dtgs detector.

3. RESULTS AND DISCUSSION

3.1. Crystal Structures. The structures of the complexes were determined by single-crystal X-ray diffraction. Crystallographic data and structure refinement parameters are summarized in Table 2.

Compound **1**, $Ce(HCOO)_3$, crystallizes in the trigonal space group *R*3*m* with Z = 3. The structure has thus a 3-fold rotation symmetry. The Ce(III) atoms of $Ce(HCOO)_3$ are 9-fold coordinated (see Figure 1). A list of bond lengths is given in the Supporting Information, Table S1. The coordination polyhedron of the Ce(III) cation is a tricapped trigonal prism. The Ce–O distances of the capping oxygens (O1) are 2.583(8) and 2.601(8) Å, whereas the equatorial Ce–O distances are 2.506(9) Å. There exists only one symmetry-independent $HCOO^-$ molecule in the structure. One oxygen atom (O1) binds to two neighboring Ce(III) atoms by forming infinite linear chains along the [001] direction (Figure 1). The other oxygen atom (O2) of the carboxylic group forms a monodentate bond with a Ce(III) atom on the equatorial plane of the coordination polyhedron. As a whole, the $HCOO^-$ molecule acts as a tridentate ligand. The Ce(III) chains are

dx.doi.org/10.1021/ic400999j | *Inorg. Chem.* 2013, 52, 11734–11743

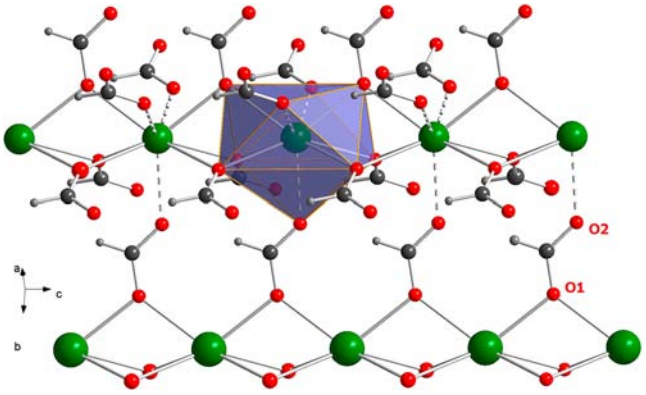

Figure 1. Structure of complex **1**, $Ce(HCOO)_3$. Color code: Ce green, O red, C large gray spheres, H small gray spheres. The blue polyhedron highlights the Ce(III) coordination polyhedron. The Ce–Ce distance is 4.1205(12) Å.

exclusively bridged by the $HCOO^-$ ligands. Counter ions are not involved in the structure.

The complex structure **2**, $[Ce_6(\mu_3\text{-}O)_4(\mu_3\text{-}OH)_4(HCOO)_{10}(NO_3)_2(H_2O)_3]\cdot(H_2O)_{9.5}$, consists of a hexanuclear Ce(IV) formate complex (Figure 2). A list of bond

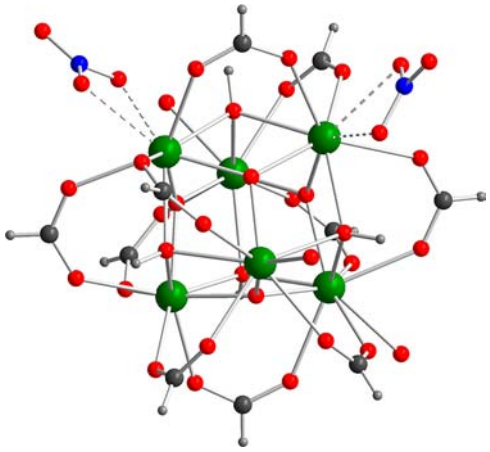

Figure 2. Structure of **2**, $[Ce_6(\mu_3\text{-}O)_4(\mu_3\text{-}OH)_4(HCOO)_{10}(NO_3)_2(H_2O)_3]\cdot(H_2O)_{9.5}$ (counterions are omitted for clarity). Color code: Ce green, O red, N blue, C large gray spheres, H small gray spheres.

lengths is given in the Supporting Information, Table S2. Six Ce(IV) atoms in the hexanuclear core $[Ce_6(\mu_3\text{-}O)_4(\mu_3\text{-}OH)_4]^{12+}$ are arranged at the corners of a nearly regular octahedron with Ce–Ce distances ranging from 3.7183(5) to 3.8252(6) Å. The eight faces of the octahedron are bridged by either μ_3-O or μ_3-OH oxygen atoms, resulting in four μ_3-O and four μ_3-OH bridging units in a single hexanuclear core. The type of bridging oxygen, that is, oxo or hydroxo, was identified by their Ce–O bond lengths, which range from 2.172(4) to 2.260(4) Å for the μ_3-O, and from 2.395(4) to 2.620 (5) Å for the μ_3-OH. The oxo and hydroxo oxygen atoms are alternatingly arranged: each of the μ_3-O has three μ_3-OH neighbors, and each μ_3-OH has three μ_3-O neighbors. Ten out of the 12 edges of the octahedron are bridged by the carboxylic group of the $HCOO^-$ ligands through a *syn-syn* coordination as shown in Figure 2. Actinide (An) complexes with Th(IV) and U(IV) show similar hexanuclear structures with 12 $HCOO^-$ ligands regularly bridging the 12 edges of the $[An_6(\mu_3\text{-}O)_4(\mu_3\text{-}OH)_4]^{12+}$octahedron.[28] Structure **2** differs from this regular ligand arrangement, as two NO_3^- groups are replacing formate ligands. However, the 10 $HCOO^-$ and 2 NO_3^- ligands compensate the charge of the $[Ce_6(\mu_3\text{-}O)_4(\mu_3\text{-}OH)_4]^{12+}$ core. The Ce(IV) hexanuclear complex has three terminal water molecules. Each Ce(IV) ion is bound to two μ_3-O and two μ_3-OH. Three out of the six Ce(IV) atoms show a coordination number of 8 (either 4 $HCOO^-$; or 3 $HCOO^-$ and 1 H_2O in addition to 2 μ_3-O and 2 μ_3-OH), the other three Ce(IV) show a coordination number of 9 (either 4 $HCOO^-$ and 1 H_2O; or alternatively 3 $HCOO^-$ and 1 NO_3^- in addition to 2 μ_3-O and 2 μ_3-OH). This is an indication that the ionic radius of Ce(IV) is just at the limit to stabilize either a coordination of 8 or 9, whereas the so far known tetravalent actinide carboxylates show exclusively a coordination number of 9. There are no charge compensating counterions present in the structure. The space between the hexanuclear complexes is filled solely by water molecules.

Structure **3**, $[Ce_6(\mu_3\text{-}O)_4(\mu_3\text{-}OH)_4(HCOO)_{10}(NO_3)_4]\cdot(NO_3)_3(NH_4)_5(H_2O)_5$, crystallizes in the orthorhombic space group *Pbcn*. Because of the high symmetry, the asymmetric unit consists only of the half cluster. This complex structure is similar to structure **2** and consists of the same hexanuclear core $[Ce_6(\mu_3\text{-}O)_4(\mu_3\text{-}OH)_4]^{12+}$ with the same arrangement of the four μ_3-O and four μ_3-OH (Figure 3). A list of bond lengths is

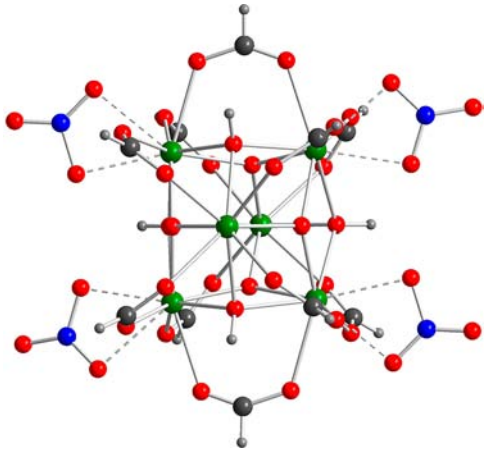

Figure 3. Structure of **3**, $[Ce_6(\mu_3\text{-}O)_4(\mu_3\text{-}OH)_4(HCOO)_{10}(NO_3)_4]\cdot(NO_3)_3(NH_4)_5(H_2O)_5$ (counterions are omitted for clarity). Color code: Ce green, O red, N blue, C large gray spheres, H small gray spheres.

given in the Supporting Information, Table S3. The similarity of the hexanuclear core includes the Ce–O bond lengths of the oxo and hydroxo groups, ranging from 2.150(6) to 2.261(7) Å for the μ_3-O, and from 2.384(5) to 2.481(6) Å for the μ_3-OH. Another similarity is that 10 out of the 12 edges of the octahedron are bridged by the carboxylic group of the $HCOO^-$ ligands through a *syn-syn* coordination as shown in Figure 3. A significant difference is that structure **3** does not show any terminating H_2O molecule, but there are 4 NO_3^- ligands in bidentate coordination. The chelating 10 $HCOO^-$ and 4 NO_3^- ligands and the $[Ce_6(\mu_3\text{-}O)_4(\mu_3\text{-}OH)_4]^{12+}$ core balance the charge to a total charge of 2–. This negative charge is compensated by NH_4^+ counterions. Two out of the six Ce(IV) atoms show a coordination number of 8 (2 μ_3-O, 2 μ_3-OH, and 4 $HCOO^-$) and four Ce(IV) show a coordination number of 9

dx.doi.org/10.1021/ic400999j | *Inorg. Chem.* 2013, 52, 11734–11743

(2 μ_3-O, 2 μ_3-OH, 3 $HCOO^-$, and 2 oxygen atoms from a bidentate NO_3^-). In the space between the hexanuclear complexes are, furthermore, 2 NO_3^- groups arranged whose charge is compensated by NH_4^+. Short distances related with potential hydrogen bridges are shown in Supporting Information, Figure S6.

The hydrogen atoms in this crystal structure could not be located experimentally. The charge balance would be uncertain if both the hexanuclear cluster and the counterions contain hydrogen atoms which could not be identified experimentally. The charge of the hexanuclear cluster is neutralized by NH_4^+. However, it is difficult to distinguish the electron density of the nitrogen atoms in NH_4^+ explicitly from that of the oxygen atoms in H_2O. Although precaution has taken to keep Ce(IV) stable, evidence is required that the synthesis did not result in a Ce(III)/Ce(IV) mixed-valent crystal structure. The oxidation state of cerium can be verified by analyzing the Ce L_3-edge XANES (Figure 4). The Ce L_3-edge spectrum of Ce(III)

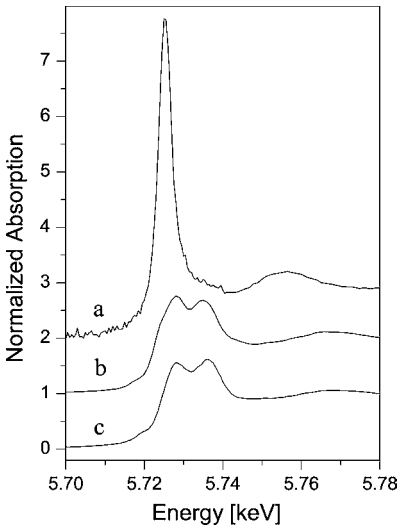

Figure 4. Ce L_3-edge XANES spectra of (a) Ce(III) reference of 0.01 M Ce(III) nitrate in H_2O, (b) Ce(IV) reference of CeO_2, and (c) solid sample **3**. Ce K-edge XANES of the compounds are shown in the Supporting Information, Figure S7.

consists of a single peak just above the absorption threshold associated with the electron transition $2p^64f^1(5d,6s)^3 \rightarrow 2p^54f^1(5d,6s)^4$. The Ce L_3-edge spectrum of Ce(IV) shows two resonances whose origin is interpreted as a result of mixed state between f^0 and f^1L[29] or alternatively as an almost pure f^0 state[30,31] with a peak at higher energy following the transition $2p^64f^0(5d,6s)^4 \rightarrow 2p^54f^0(5d,6s)^5$. The energy difference between the resonances and the characteristic transition intensities is often used to determine the valence of Ce or the ratio of Ce(III)/Ce(IV) in mixed-valent systems.[32−35] An aqueous solution of 0.01 M Ce(III) nitrate was used as reference for Ce(III), while CeO_2 was used as reference for Ce(IV). The L_3-edge XANES spectrum of sample **3** shows essentially the same spectral features as those observed for the Ce(IV) reference. The presence of Ce(III) can be therefore excluded in sample **3**.

The formation of the hexanuclear Ce(IV) formate complexes corresponds with the Ce(IV) hydrolysis and the deprotonation of HCOOH in the same pH region. The Ce(IV) hydrolysis results in an oligomerization through oxo and hydroxo bonds, whereas the carboxylic function of formate introduces chelating ligands, stabilizing the hexanuclear oligomer.

Despite several attempts we were so far not successful in obtaining the Ce(IV) formate complex without nitrate coordination. Nitrate was used in the synthesis because it supports the stability of Ce(IV) in aqueous solution most likely through complex formation.[36,37] As a matter of fact, the crystal preparation of Ce(IV) formate complexes in perchlorate and chloride media only results in the reduction of Ce(IV) to Ce(III) just a few hours after the preparation of mother Ce(IV) solutions. The hexanuclear $[Ce_6(\mu_3\text{-}O)_4(\mu_3\text{-}OH)_4]^{12+}$ core in sample **2** and **3** is stabilized by the *syn-syn* coordinated carboxylic groups of formate, whereas nitrate acts not as such chelating ligand. It should be mentioned that sulfate, which also supports Ce(IV) stability through complex formation,[38] can act as chelating ligand resulting in hexanuclear $[Ce_6(\mu_3\text{-}O)_4(\mu_3\text{-}OH)_4(SO_4)_6]$ units.[39] There are hexanuclear Ce(IV) structures known with exclusive coordination of 12 carboxylic and other functional groups, such as the hexanuclear complex $[Ce_6(\mu_3\text{-}O)_4(\mu_3\text{-}OH)_4(acac)_{12}]$, acac = acetylacetonate,[40] and $[Ce_6(\mu_3\text{-}O)_4(\mu_3\text{-}OH)_4(\mu_2\text{-}O_2C^tBu)_{12}]$, O_2C^tBu = pivalate *t*-Bu.[41] It is interesting to note that the above-mentioned hexanuclear Ce(IV) carboxylates do not comprise an interstitial μ_6-oxo oxygen atom. Such a μ_6-oxo oxygen atom at the center of the octahedron was observed in several hexanuclear trivalent lanthanide (Ln) clusters forming the unit $[Ln_6(\mu_6\text{-}O)_4(\mu_3\text{-}OH)_8]^{8+}$, where the μ_6-O is believed to play a role in stabilizing the hexanuclear core.[42,43] Such hexanuclear La(III) clusters can also involve bidentately coordinating terminal nitrate groups,[44] in a similar manner as observed for the compounds **2** and **3**. The competing coordination of carboxylic ligands of benzoate and nitrate has been observed in the hexanuclear cluster $[Ce_6(\mu_3\text{-}O)_5(\mu_3\text{-}OH)_3(C_6H_5COO)_9(NO_3)_3(DMF)_3]$.[45]

3.2. Solution Species. Subsequently we investigate the coordination of Ce(III) and Ce(IV) formate complexes in aqueous solution with Ce K-edge EXAFS spectroscopy.

3.2.1. Ce(III) Formate. To verify the structural difference between the Ce(III) formate complexes in aqueous solution and the Ce(III) aquo species itself, a reference sample of 0.1 M $Ce(NO_3)_3{\cdot}6H_2O$ in H_2O at pH 2 (sample **A1**) was investigated. Such aquo species, $Ce^{3+}(aq)$, are supposed to be coordinated by 9 water molecules in a tricapped trigonal prism fashion, which can be formulated as $Ce(H_2O)_9^{3+}$.[3,4] The EXAFS spectrum of this sample (Figure 5), shows 9.4(3) oxygen atoms from water at a Ce−O distance of 2.522(2) Å.

As a second reference a solid powder of $Ce(HCOO)_3$ was investigated (sample **P1**). In this structure all formate ligands appear in monodentate coordination (Figure 1). The EXAFS spectrum (Figure 5) shows 9 oxygen atoms at an average Ce−O distance of 2.523(2) Å, a broad peak originated from Ce−C scattering pairs at 3.431(8) and 3.601(6) Å, and furthermore the nearest Ce neighbors in the linear Ce(III) chain at a Ce−Ce distance of 4.100(2) Å. Infinite linear chains in structure **1** are formed during the crystallization process, while they are not expected to exist in solution. Nevertheless, the solution species may occur either as mononuclear species or as a preshaped polynuclear precursor.

To obtain the structural information on a Ce(III) formate complex in solution, $Ce(HCOO)_3$ from sample **P1** was dissolved in water (sample **A2**). The pH value of this colorless solution approached 5.74 without further adjustment. Concentrations of higher than ~0.025 M Ce(III) resulted in precipitation, indicating that the present Ce(III) formate solution ([Ce] = 0.018 M) is close to the solubility limit. The reported stability constants of Ce(III) formate suggest the

dx.doi.org/10.1021/ic400999j | Inorg. Chem. 2013, 52, 11734−11743

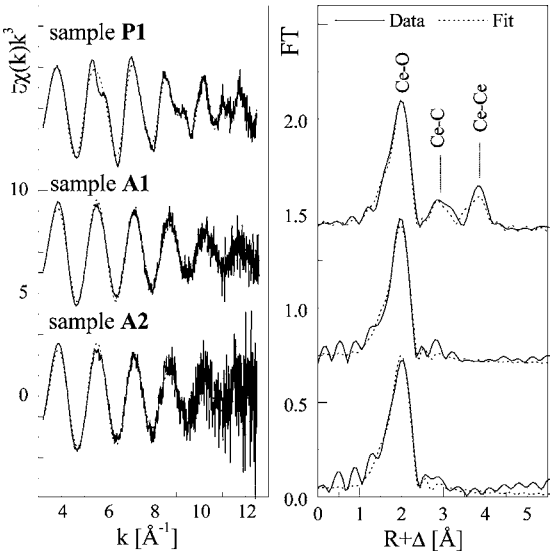

Figure 5. Ce K-edge k^3-weighted EXAFS data (left) and the corresponding Fourier transforms (right) of solid $Ce(HCOO)_3$ (sample **P1**), aqueous solution of 0.1 M $Ce(NO_3)_3{\cdot}6H_2O$ in H_2O at pH 2.0 (sample **A1**), and 0.018 M $Ce(HCOO)_3$ in H_2O at pH 5.74 (sample **A2**).

presence of two stable species: $Ce(HCOO)^{2+}$ with log β_1 = 1.79 and $Ce(HCOO)_2^+$ with log β_2 = 2.97.[10,19,20] These stability constants were used to estimate the species distribution as a function of pH (see Supporting Information, Figure S8). According to that estimate, the Ce(III) species of sample **A2** are composed of 42% Ce^{3+}(aq), 41% $Ce(HCOO)^{2+}$, and 17% $Ce(HCOO)_2^+$. The EXAFS spectrum of this sample is shown in Figure 5. The spectrum reveals only a single peak of 9.6(3) O atoms at a Ce−O distance of 2.521(2) Å (Table 3). It is expected from the single crystal data that the Ce−O distance between Ce(III) and the monodentately coodinating $HCOO^-$ is also around 2.52 Å (Table 3, Solid sample **P1**), which is identical to that of Ce−O(H_2O) (Table 3, solution **A1**). There is no significant difference in the Ce−O distance and the coordination number between the Ce(III) aquo complex and solution with Ce(III) formate. It should be mentioned that EXAFS is not sensitive to individual solution species and provides an average scattering signal. The absence of further significant peaks in the spectrum of sample **A2** prevents a detailed interpretation of the $HCOO^-$ coordination. It can be summarized that the Ce(III) formate species in aqueous solutions are monomeric complexes as can be indicated from the absence of a Ce−Ce scattering contribution.

3.2.2. Ce(IV) Formate. The electrolysis of 0.12 M Ce(III) in 0.56 M HNO_3 results in the formation of Ce(IV). This initial solution (sample **Init**) shows an intense yellow color. The addition of formic acid into this solution does not result in a significant color change. In the course of the titration of the Ce(IV) formate solution (sample **F1**) with NH_3 the color of the solution fades out first, and then turns into a pale yellow (a photo of the complete sample series is shown in Supporting Information, Figure S9. The oxidation state of Ce(IV) remains unchanged over the whole sample series as verified by Ce K-edge XANES spectra (see Supporting Information, Figure S10. The color change is thus an effect of complex formation between Ce(IV) and formate.

The successive complex formation associated with the titration was investigated by Ce K-edge EXAFS spectroscopy (Figure 6). The Fourier transform of the initial solution

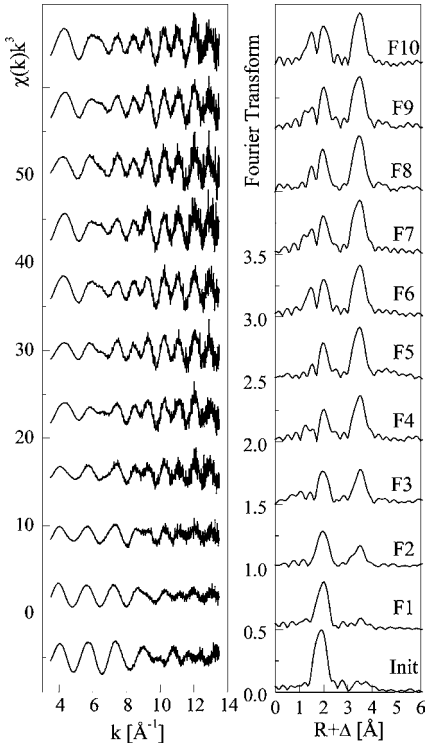

Figure 6. Ce *K*-edge k^3-weighted EXAFS data (left) and the corresponding Fourier transforms (right) of aqueous solutions with 0.01 M Ce(IV), 0.5 M HNO_3, and 1 M HCOOH with different pH values. The sample composition is listed in Table 1

Table 3. EXAFS Fit Parameters of Solid $Ce(HCOO)_3$ (Sample P1), Aqueous Solution of 0.1 M $Ce(NO_3)_3{\cdot}6H_2O$ in H_2O at pH 2.0 (Sample A1), and 0.018 M $Ce(HCOO)_3$ in H_2O at pH 5.74 (Sample A2)

sample	scattering path	R/Å	N	σ^2/Å^2	$\Delta E_{k=0}$ / eV	F
solid sample **P1**	Ce−O	2.523(2)	9[a]	0.0084(1)	0.4(3)	0.11
	Ce−C1	3.431(8)	6[a]	0.0047(7)		
	Ce−C2	3.601(6)	3[a]	0.0032(6)		
	Ce−Ce	4.100(2)	2[a]	0.0062(3)		
solution **A1**	Ce−O	2.522(2)	9.4(3)	0.0085(3)	0.8(4)	0.28
solution **A2**	Ce−O	2.521(2)	9.6(3)	0.0089(4)	1.9(3)	0.78

[a]Coordination numbers are taken from the crystallographic data of the solid sample **1** and fixed during the fit procedure. Standard deviations are given in parentheses. Errors in distances R are ±0.02 Å, errors in coordination numbers are ±15%.

dx.doi.org/10.1021/ic400999j | *Inorg. Chem.* 2013, 52, 11734−11743

(sample **Init**) shows a dominant peak at $R + \Delta \sim 1.9$ Å. The EXAFS spectrum changes with addition of formic acid (sample **F1**) in the higher k-range ($k > 9$ Å^{-1}). During the titration with NH_3 the series of spectra shows a systematic change of their spectral features: the dominant peak at $R + \Delta \sim 1.9$ Å becomes split, and a new peak appears at $R + \Delta \sim 3.5$ Å. The new peak in the last sample of the series (sample **F10**) corresponds to 4 Ce neighbors with a Ce−Ce distance of 3.790(3) Å. This indicates the formation of a polynuclear Ce(IV) formate complex.

The Ce K-edge EXAFS spectra and the structure parameters of solution sample **F10** with the most evolved polynuclear species were compared with those of the solid $[Ce_6(\mu_3\text{-}O)_4(\mu_3\text{-}OH)_4(HCOO)_{10}(NO_3)_4]\cdot(NO_3)_3(NH_4)_5(H_2O)_5$ (sample **3**) in Figure 7 and Table 4. The spectral shape of the EXAFS

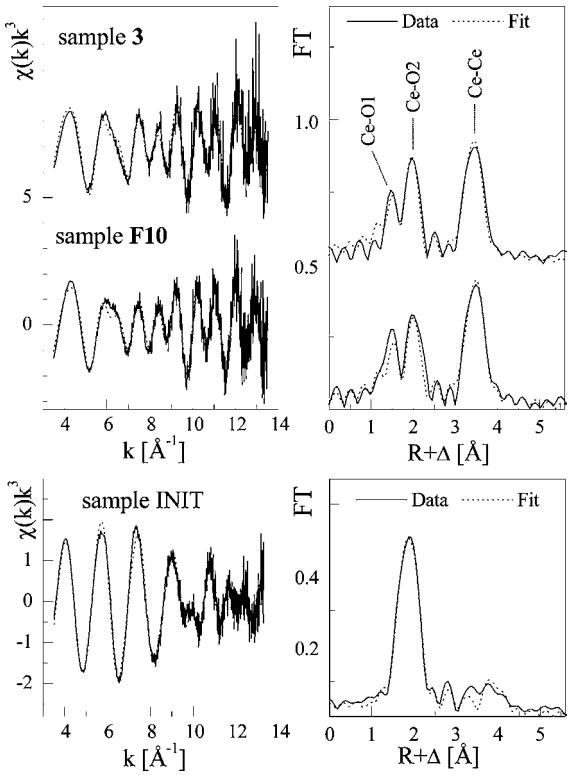

Figure 7. Top: Ce K-edge k^3-weighted EXAFS data (left) and the corresponding Fourier transforms (right) of the solid hexanuclear Ce(IV) formate (sample **3**) and the aqueous solution of 0.1 M Ce(IV) in 1 M HCOOH at pH 3.5 (sample **F10**). Bottom: Ce K-edge EXAFS and Fourier transforms of 0.1 M Ce(IV) in 0.5 M HNO_3 (sample **Init**).

oscillation, their Fourier transforms, and fit parameters are almost identical, suggesting that the polynuclear complex structure of the solution species is essentially the same as that of the solid hexanuclear Ce(IV) formate complex. The splitting of the oxygen shells results from the different Ce−O bond lengths of the μ_3-O and μ_3-OH oxygens in the $[Ce_6(\mu_3\text{-}O)_4(\mu_3\text{-}OH)_4]^{12+}$ unit and the oxygen atoms of the chelating $HCOO^-$ unit. This splitting has been observed as a characteristic effect in EXAFS spectra of analogous hexanuclear carboxylate complexes of tetravalent actinides.[28,46,47] In general, crystal structures of tetravalent actinides show similar hexanuclear $[An_6(\mu_3\text{-}O)_4(\mu_3\text{-}OH)_4]^{12+}$ complexes in presence of carboxylates.[28,47,48] The scattering contribution of possibly coordinated nitrate groups is below the detection limit. It can be concluded that the Ce(IV) forms a hexanuclear species in solution whose main coordination features remain preserved during the crystallization process. This solution species can be described generally as $[Ce_6(\mu_3\text{-}O)_4(\mu_3\text{-}OH)_4(HCOO)_x(NO_3)_y]^{12-x-y}$.

There is wide agreement in the literature that a Ce(IV) nitrate solution as in sample **Init** is composed of polymeric species, mainly dimers and trimers.[36,38b,49,50] The EXAFS spectrum of sample **Init** shows several peaks in the range $R + \Delta = 2.5$−4.0 Å. The peaks may originate from Ce−Ce interaction, nitrate ions, and/or water molecules. Possible scattering contributions from NO_3^- have been investigated. For comparison, the EXAFS spectrum, fit parameters, and the coordination polyhedron of the mononuclear $[Ce(NO_3)_6]^{2-}$ anion is given in the Supporting Information, Figures S11−S12 and Table S4. The presence of bidentate coordinated nitrate in the coordination sphere is supported by the existence of the solid Ce(IV) nitrate dimer $Ce_2O(NO_3)_6(H_2O)_6\cdot 2H_2O$.[51] The Fourier transform of bidentate coordinated nitrate is commonly dominated by the multiple scattering peak at $R + \Delta \sim 3.7$ Å (see Supporting Information, Figure S12). A peak also appears in sample **Init** at $R + \Delta \sim 3.7$ Å, but not with dominating intensity as in case of the above mentioned nitrate. The EXAFS data reveals furthermore Ce−Ce interactions. There is a striking similarity between the Ce−Ce distances of sample **Init** and the ones discussed for Ce(IV) in $HClO_4$.[6] The Ce−Ce distance of 3.284(4) Å of sample **Init** is close to the Ce−Ce distance of the trimer $[Ce_3(\mu_2\text{-}O)_3(\mu_3\text{-}O)_2(H_2O)_{12}]^{2+}$, whereas the Ce−Ce distance of 4.180(3) Å corresponds well with that in the single-oxo bridging dimer $[Ce_2(\mu_2\text{-}O)(H_2O)_{14}]^{6+}$. The structure models obtained from density functional theory (DFT) calculations in ref 6 are shown in the Supporting Information, Figure S13. The scattering signal of nitrate in sample **Init** is weak in relation to the Ce−Ce scattering contribution and is not considered in the data fit. The molar fraction of the polymers in the sample can be obtained from the coordination numbers of the trimers and dimers. The trimers have two backscattering atoms; thus, the coordination number 0.4(1) results in a mole fraction of 0.2 trimers. Dimers have one backscattering atom, and the coordination number 0.9(1) is identical with the mole fraction. It can be concluded that dimeric species are predominant in sample **Init**. The most likely dominating dimeric solution species can be described as $[Ce_2(\mu_3\text{-}O)_a(\mu_3\text{-}OH)_b(NO_3)_c]^{8-2a-b-c}$. Water molecules carry no charge and are not explicitly noted in the formula.

The EXAFS data of the sample series was further investigated with factor analysis to estimate how many significant solution species appear during the titration process. The analysis reveals two main components. The limiting spectra of these components are essentially identical with the spectra of the first (**Init**) and the last (**F10**) samples of the series, that is, the species $[Ce_2(\mu_3\text{-}O)_a(\mu_3\text{-}OH)_b(NO_3)_c]^{8-2a-b-c}$ and $[Ce_6(\mu_3\text{-}O)_4(\mu_3\text{-}OH)_4(HCOO)_x(NO_3)_y]^{12-x-y}$. Further components could not be extracted. It should be mentioned that factor analysis is sensitive to the experimental noise and may not reproduce minor components. Figure 8 shows the quantitative component distribution in the samples. It is obvious that the development of the final complex (red) is not finished at pH 0.60 (sample **F4**) where the pH value reaches its minimum. The complex appears to be approximately 100% at pH ≥ 1.16 (sample **F7**). Figure 8 reveals that with addition of HCOOH to the initial solution (sample **F1**), already 20% of Ce(IV) appear

dx.doi.org/10.1021/ic400999j | Inorg. Chem. 2013, 52, 11734−11743

Table 4. EXAFS Fit Parameters of the Solid Hexanuclear Ce(IV) Formate (Sample 3), and Aqueous Solutions of 0.1 M Ce(IV) in 1 M HCOOH at pH 3.5 (Sample F10) and 0.1 M Ce(IV) in 0.5 M HNO_3 (Sample Init)[a]

sample	scattering path	R/Å	N	σ^2/Å^2	$\Delta E_{k=0}$ / eV	F
solid sample **3**	Ce−O1	2.193(6)	2[b]	0.0052(5)	−1.1(3)	0.45
	Ce−O2	2.392(4)	6[b]	0.0078(4)		
	Ce−Ce	3.771(3)	4[b]	0.0064(1)		
solution **F10**	Ce−O1	2.191(5)	2[b]	0.0054(4)	1.2(4)	0.29
	Ce−O2	2.402(5)	6[b]	0.0095(4)		
	Ce−Ce	3.790(3)	4[b]	0.0062(1)		
solution **Init**	Ce−O1	2.063(3)	0.9(4)	0.0054(3)	−0.7(2)	0.33
	Ce−O2	2.462(3)	8.2(3)	0.0112(3)		
	Ce−Ce1	3.284(4)	0.4(1)	0.0066(8)		
	Ce−Ce2	4.180(3)	0.9(1)	0.0049(7)		

[a]The spectra are shown in Figure 7. [b]Coordination numbers are taken from the crystallographic data of the solid sample and fixed during the fit procedure. Standard deviations are given in parentheses. Errors in distances R are ±0.02 Å, errors in coordination numbers are ±15%. The scattering signal of nitrate is weak in relation to the Ce−Ce scattering contribution and is therefore not considered in the fit.

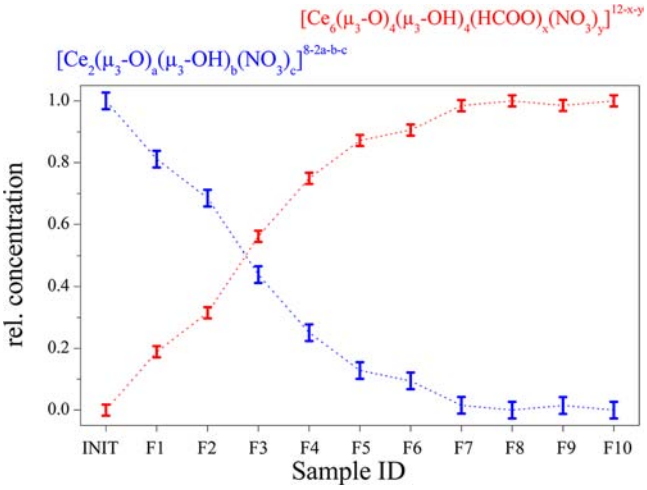

Figure 8. Relative concentrations of the two components obtained by factor analysis of EXAFS spectra shown in Figure 6. The blue color represents the initial species, while the red color represents the hexanuclear Ce(IV) formate complex. The spectra of the extracted components are shown in the Supporting Information, Figure S14.

as hexanuclear Ce(IV) formate. With increasing volume of NH_3 the relative concentration of hexanuclear Ce(IV) formate species approaches 100%.

Assuming that, in the present Ce(IV)-formate aqueous solution system, the initial precursor species of oxo/hydroxo-bridging dinuclear complexes have evolved into the hexanuclear complexes, the following three main chemical equilibria are expected to occur during the pH titration process:

$$NH_3 + H_2O \leftrightarrow NH_4^+ + OH^- \quad (1)$$

$$HCOOH \leftrightarrow HCOO^- + H^+ \quad (2)$$

$$3[Ce_2(\mu_3\text{-}O)_a(\mu_3\text{-}OH)_b(NO_3)_c]^{8-2a-b-c} + xHCOO^- + (y - 3c)NO_3^- + (8 - 3a - 3b)H_2O \leftrightarrow [Ce_6(\mu_3\text{-}O)_4(\mu_3\text{-}OH)_4(HCOO)_x(NO_3)_y]^{12-x-y} + (12 - 6a - 3b)H^+ \quad (3)$$

Based on the results of factor analysis on EXAFS data (Figure 8), we assume that the hexanuclear Ce(IV) complexes, $[Ce_6(\mu_3\text{-}O)_4(\mu_3\text{-}OH)_4(HCOO)_x(NO_3)_y]^{12-x-y}$, are constantly formed during the titration process. The addition of NH_3 results in a release of OH^- ions (Reaction 1), promotes the dissociation of HCOOH to $HCOO^-$ (Reaction 2), and consequently, accelerates the evolution of the precursor Ce(IV) dinuclear complexes into the hexanuclear complexes via Reaction 3. This means that the addition of the base in the system triggers the formation of the hexanuclear Ce(IV) formate complexes with a byproduct of $(12 - 6a - 3b)H^+$, where the sum $a + b$ is expected to be less than 3.[6] As indicated in Table 1, the initial stage of titration of the Ce(IV)-formate solution with NH_3 results in the decrease in pH despite the addition of the basic reagent. This could be interpreted as a result of this excess production of $(12 - 6a - 3b)H^+$. After reaching pH 0.60 (sample **F4**), where approximately 80% of Ce(IV) species are present as the hexanuclear complexes (Figure 8), the deprotonation of HCOOH to $HCOO^-$, which is driven by the addition of NH_3 (Reactions 1 and 2), weakens considerably and, consequently, the formation of the hexanuclear complexes is already nearly complete and the release of H^+ is lowered. In consequence, the H^+ production through the formation of hexanuclear complex does not overwhelm the volume of the added base any longer, finally increasing pH from sample **F4** toward sample **F10**.

4. CONCLUSION

Ce−K edge EXAFS spectra of an aqueous solution of Ce(III) formate, where thermodynamic stability constants predict the presence of $Ce(HCOO)^{2+}$ and $Ce(HCOO)_2^+$, show the presence of monomeric Ce(III) complexes. Only microcrystalline precipitates with the composition $Ce(HCOO)_3$ were obtained from the same Ce(III) formate solution and used for EXAFS measurement. Single crystals of $Ce(HCOO)_3$ could be obtained from an equivalent Ce(IV) solution through slow photoreduction of Ce(IV) to Ce(III). The solution species undergo a polymerization and result in a crystal structure with linear Ce−3O−Ce chains. The Ce(III) in the crystal structure is exclusively coordinated by $HCOO^-$ ligands in a monodentate fashion.

Increasing pH in aqueous solutions of Ce(IV) formate leads to the formation of a hexanuclear complex with an $[Ce_6(\mu_3\text{-}O)_4(\mu_3\text{-}OH)_4]^{12+}$ core, being bridged by $HCOO^-$ and NO_3^- ligands to form $[Ce_6(\mu_3\text{-}O)_4(\mu_3\text{-}OH)_4(HCOO)_x(NO_3)_y]^{12-x-y}$. Single crystals were obtained in the stability range of this solution species. The hexanuclear solution species remains preserved in the crystal structure. Consequently, from such

dx.doi.org/10.1021/ic400999j | Inorg. Chem. 2013, 52, 11734−11743

solutions crystallizes a compound with the composition $[Ce_6(\mu_3\text{-}O)_4(\mu_3\text{-}OH)_4(HCOO)_{10}(NO_3)_4]\cdot(NO_3)_3(NH_4)_5(H_2O)_5$ including four nitrate ligands in the hexanuclear complex. Using different titration agents (NH_3 or NaOH) yields slightly different hexanuclear Ce(IV) formate complexes. A titration with NaOH resulted in the formation of a hexanuclear complex with the composition $[Ce_6(\mu_3\text{-}O)_4(\mu_3\text{-}OH)_4(HCOO)_{10}(NO_3)_2(H_2O)_3]\cdot(H_2O)_{9.5}$ with two nitrate ligands in the hexanuclear complex.

The different structures observed for Ce(III) and Ce(IV) reflect the different influence of hydrolysis. In case of Ce(III) the hydrolysis occurs far above the onset of the formation of formate complexes at pH ∼ 2. In case of Ce(IV) hydrolyzed polynuclear species already appear in an acidic solution without the addition of basic reagents. The polynuclear Ce(IV) formate complex appears thus from a competing reaction between hydrolysis and ligation. The hydrolysis causes polymerization through olation and oxolation, while the ligation by the carboxylic groups of $HCOO^-$ prevents further hydrolytic polymerization and, consequently, stabilizes the hexanuclear complex in an aqueous solution.

■ ASSOCIATED CONTENT

Supporting Information

Experimental details, X-ray diffraction data (single crystals and powder), species fraction in solution, XANES and EXAFS spectra and structural parameters, photos of the aqueous solutions, cif files of the crystal structures. This material is available free of charge via the Internet at http://pubs.acs.org.

■ AUTHOR INFORMATION

Corresponding Author

*E-mail: hennig@esrf.fr.

Notes

The authors declare no competing financial interest.

■ ACKNOWLEDGMENTS

The authors are thankful to Wouter Van Beek/SNBL for support during some EXAFS measurements and A. Scholz/HZDR and J. Wenzel/BAM for powder diffraction measurements.

■ REFERENCES

(1) Binnemans, K. Application of tetravalent cerium compounds. In *Handbook on the Physics and Chemistry of Rare Earths*; Geschneider, K. A., Jr., Bünzli, J.-C. G., Pecharsky, V. K., Eds.; Elsevier: Amsterdam, The Netherlands, 2006; Vol. *36*, pp 281−392.

(2) Richens, D. T. *The Chemistry of Aqua Ions*; John Wiley & Sons: Chichester, U.K., 1997.

(3) Habenschuss, A.; Spedding, F. H. *J. Chem. Phys.* **1980**, *73*, 442−450.

(4) Buzko, V.; Sukhno, I.; Polushin, A. *Int. J. Quantum Chem.* **2011**, *111*, 2705−2711.

(5) Baes, Jr., C. F.; Mesmer, R. E. *The Hydrolysis of Cations*; John Wiley & Sons: New York, 1976; Chapter 7, pp 138−146.

(6) Ikeda-Ohno, A.; Tsushima, S.; Hennig, C.; Yaita, T.; Bernhard, G. *Dalton Trans.* **2012**, *41*, 7190−7192.

(7) Ikeda-Ohno, A.; Hennig, C.; Weiss, S.; Yaita, T.; Bernhard, G. *Chem.—Eur. J.* **2013**, *19* (23), 7348−7360.

(8) Wadsworth, E.; Duke, F. R.; Goetz, C. A. *Anal. Chem.* **1957**, *29*, 1824−1825.

(9) Maverick, A. W.; Yao, Q. *Inorg. Chem.* **1993**, *32*, 5626−5628.

(10) Wood, S. A. *Eng. Geol.* **1993**, *34*, 229−259.

(11) Reutemann, W.; Kieczka, H. Formic acid. In *Ullmann's Encyclopedia of Industrial Chemistry*; Wiley-VCH: Weinheim, Germany, 2011.

(12) Lü, W.; Wacker, T.; Gerbing,-Smentke, E.; Andrade, L. A.; Einsle, O. *Science* **2011**, *332*, 352−354.

(13) Grasemann, M.; Laurenczy, G. *Energy Environ. Sci.* **2012**, *5*, 8171−8181.

(14) Stubenrauch, J.; Brosha, E.; Vohs, J. M. *Catal. Today* **1996**, *28*, 431−441.

(15) Senanayake, S. D.; Mullins, D. R. *J. Phys. Chem. C* **2008**, *112*, 9744−9752.

(16) Sridharan, V.; Menéndez, J. C. *Chem. Rev.* **2010**, *110*, 3805−3849.

(17) (a) Miyajima, Y.; Ishizuka, T.; Yamamoto, Y.; Sumaoka, J.; Komiyama, M. *J. Am. Chem. Soc.* **2009**, *131*, 2657−2662. (b) Aiba, Y.; Lönnberg, T.; Komiyama, M. *Chem.—Asian. J.* **2011**, *6*, 2407−2411.

(18) Tsubota, H. B. *Chem. Soc. Jpn.* **1962**, *35*, 640−644.

(19) Kovar, L. E.; Powell, J. E. *Stability constants of rare earths with some weak carboxylic acids*; Report TID-4500; Ames Laboratory, Iowa State University: Ames, Iowa, 1966.

(20) Martell, A. E.; Smith, R. M. *NIST critically selected stability constants of metal complexes*; NIST standard reference database 46, Vers. 8.0; National Institute of Standards and Technology : Gaithersburg, MD, 2004.

(21) Bolotovsky, R. L.; Bulkin, A. P.; Krutov, G. A.; Kudryashev, V. A.; Trunov, V. A.; Ulyanov, V. A.; Antson, O.; Hiismäki, P.; Pöyry; Tiitta, A.; Loshmanov, A. A.; Furmanova, N. G. *Solid State Commun.* **1990**, *76*, 1045−1049.

(22) Go, Y. B.; Jacobson, A. J. *Chem. Mater.* **2007**, *19*, 4702−4709.

(23) (a) Sheldrick, G. M. *SHELXS-97, Program for the Solution of Crystal Structures*; Universität Göttingen: Göttingen, Germany, 1997; (b) Sheldrick, G. M. *SHELXL-97, Program for the Crystal Structure Refinement*; Universität Göttingen: Göttingen, Germany, 1997.

(24) Ressler, T. *J. Synchrotron Radiat.* **1998**, *5*, 118.

(25) George, G. N.; Pickering, I. J. *EXAFSPAK, a suite of computer programs for analysis of X-ray absorption spectra*; Stanford Synchrotron Radiation Laboratory: Stanford, CA, 2000.

(26) Ankudinov, A. L.; Ravel, B.; Rehr, J. J.; Conradson, S. D. *Phys. Rev. B* **1998**, *58*, 7565−7576.

(27) (a) Rossberg, A.; Reich, T.; Bernhard, G. *Anal. Bioanal. Chem.* **2003**, *376*, 631−638. (b) Malinowski, E. R. *Anal. Chim. Acta* **1980**, *122*, 327−330.

(28) Takao, S.; Takao, K.; Kraus, W.; Emmerling, F.; Scheinost, A. C.; Bernhard, G.; Hennig, C. *Eur. J. Inorg. Chem.* **2009**, 4771−4775.

(29) (a) Kotani, A.; Ogasawara, H.; Okada, K.; Thole, B. T.; Sawatzky, G. A. *Phys. Rev. B* **1989**, *40*, 65−73. (b) Kotani, A.; Kvashnina, K. O.; Butorin, S. M.; Glatzel, P. *Eur. Phys. J. B* **2012**, *85*, 257−269.

(30) Marabelli, F.; Wachter, P. *Phys. Rev. B* **1987**, *36*, 1238−1243.

(31) Hanyu, T.; Ishii, H.; Yanagihara, M.; Kamada, T.; Miyahara, T.; Kato, H.; Naito, K.; Suzuki, S.; Ishii, T. *Solid State Commun.* **1985**, *56*, 381−383.

(32) Beck, D. D.; Capehart, T. W.; Hofman, R. W. *Chem. Phys. Lett.* **1989**, *159*, 207−213.

(33) Prieto, C.; Lagarde, P.; Dexpert, H.; Briois, V.; Villain, F.; Verdaguer, M. J. *Phys. Chem. Solids* **1992**, *53*, 233−237.

(34) Antonio, M. R.; Soderholm, L. *Inorg. Chem.* **1994**, *33*, 5988−5993.

(35) Briotis, V.; Lützenkirchen-Hecht, D.; Villain, F.; Fonda, E.; Belin, S.; Griesebock, B.; Frahm, R. *J. Phys. Chem. A* **2005**, *109*, 320−329.

(36) Blaustein, B. D.; Gryder, J. W. *J. Am. Chem. Soc.* **1957**, *79*, 540−547.

(37) Miller, J. T.; Irish, D. E. *Can. J. Chem.* **1967**, *45*, 147−155.

(38) (a) Jones, E. G.; Soper, F. G. *J. Chem. Soc.* **1935**, 802−805. (b) Hardwick, T. J.; Robertson, E. *Can. J. Chem.* **1951**, *29*, 818−827. (c) Paulenova, A.; Creager, S. E.; Navratil, J. D.; Wei, Y. *J. Power Sources* **2002**, *109*, 431−438.

(39) Lundgren, G. *Ark. Kemi* **1956**, *5*, 349−363.

(40) Toledano, P.; Ribot, F.; Sanchez. *C. R. Acad. Sci. Ser. II* **1990**, *311*, 1315−1320.
(41) Mereacre, V.; Ako, M. A.; Akhtar, M. N.; Lindemann, A.; Anson, C. E.; Powell, A. K. *Helv. Chim. Acta* **2009**, *92*, 2507−2514.
(42) Wang, R.; Carducci, M. C.; Zheng, Z. *Inorg. Chem.* **2000**, *39*, 1836−1837.
(43) Mudring, A.-V.; Timofte, T.; Babei, A. *Inorg. Chem.* **2006**, *45*, 5162−5166.
(44) Calvez, G.; Daiguebonne, C.; Guillou, O.; Le Dret, F. *Eur. J. Inorg. Chem.* **2009**, 3172−3178.
(45) Das, R.; Samara, R.; Baruah, J. B. *Inorg. Chem. Commun.* **2010**, *23*, 793−795.
(46) Takao, K.; Takao, S.; Scheinost, A. C.; Bernhard, G.; Hennig, C. *Inorg. Chem.* **2012**, *51*, 1336−1344.
(47) Hennig, C.; Takao, S.; Takao, K.; Weiss, S.; Kraus, W.; Emmerling, F.; Scheinost, A. C. *Dalton Trans.* **2012**, *41*, 12818−12823.
(48) (a) Lundgren, G. *Ark. Kemi* **1952**, *5*, 421−428. (b) Morkry, L. M.; Dearn, N. S.; Carrano, C. J. *Angew. Chem., Int. Ed. Engl.* **1996**, *35*, 1497−1498. (c) Duval, P. B.; Burns, C. J.; Buschmann, W. E.; Clark, D. L.; Morris, D. E.; Scott, B. L. *Inorg. Chem.* **2001**, *40*, 5491−5496. (d) Berthet, J. C.; Thuery, P.; Ephritikhine, M. *Chem. Commun.* **2005**, 3415−3417. (e) Nocton, G.; Burdet, F.; Pecaut, J.; Mazzanti, M. *Angew. Chem., Int. Ed.* **2007**, *46*, 7574−7578. (f) Nocton, G.; Pecaut, J.; Filinchuk, Y.; Mazzanti, M. *Chem. Commun.* **2010**, *46*, 2757−2759. (g) Mougel, V.; Biswas, B.; Pecaut, J.; Mazzanti, M. *Chem. Commun.* **2010**, *46*, 8648−8650. (h) Biswas, B.; Mougel, V.; Pecaut, J.; Mazzanti, M. *Angew. Chem., Int. Ed.* **2011**, *123*, 5863−5866. (i) Knope, K. E.; Wilson, R. E.; Vasiliu, M.; Dixon, D. A.; Soderholm, L. *Inorg. Chem.* **2011**, *50*, 9696−9704. (j) Vasiliu, M.; Knope, K. E.; Soderholm, L.; Dixon, D. A. *J. Phys. Chem.* **2012**, *116*, 6917−6926. (k) Knope, K. E.; Soderholm, L. *Chem. Rev.* **2013**, *113*, 944−994. (l) Hennig, C.; Takao, S.; Takao, K.; Weiss, S.; Kraus, W.; Emmerling, F.; Meyer, M.; Scheinost, A. C. *J. Phys. Conf. Series* **2013**, *430*, 012116. (m) Falaise, C.; Volkringer, C.; Vigier, J.-F.; Henry, N.; Beaurain, A.; Loiseau, T. *Chem.—Eur. J.* **2013**, *19*, 5324−5331.
(49) Wiberg, K. B.; Ford, P. C. *Inorg. Chem.* **1968**, *7*, 369−373.
(50) Duke, F. R.; Parchen, F. R. *J. Am. Chem. Soc.* **1956**, *78*, 1540−1543.
(51) Guillou, N.; Auffrédic, J. P.; Louër, J. *Solid State Chem.* **1994**, *112*, 45−52.